LAWRENCE LIVERMORE NATIONAL LABORATORY

UCRL-CONF-203555

Preliminary Performance Measurements for a Streak Camera with a Large-Format Direct-Coupled CCD Readout

R. A. Lerche, J. W. McDonald, R. L. Griffith, G. Vergel de Dios, D. S. Andrews, A. W. Huey, P. M. Bell, O. L. Landen, P. A. Jaanimagi, R. Boni

April 16, 2004

The 15th Topical Conference on High-Temperature Plasma Diagnostics
San Diego, CA, United States
April 19, 2004 through April 22, 2004

UCRL-CONF-203555

Preliminary Performance Measurements for a Streak Camera with a Large-Format Direct-Coupled CCD Readout

R.A. Lerche, J.W. McDonald, R.L. Griffith, G.Vergel de Dios, D.S. Andrews, A.W. Huey, P.M. Bell, O.L. Landen
Lawrence Livermore National Laboratory, University of California, Livermore, California 94551

P. A. Jaanimagi, R. Boni
Laboratory for Laser Energetics, University of Rochester,250 East River Road, Rochester, NY 14523

ABSTRACT

Livermore's ICF Program has a large inventory of optical streak cameras built in the 1970s and 1980s. The cameras are still very functional, but difficult to maintain because many of their parts are obsolete including the original streak tube and image-intensifier tube. The University of Rochester's Laboratory for Laser Energetics is leading an effort to develop a fully automated, large-format streak camera that incorporates modern technology. Preliminary characterization of a prototype camera shows spatial resolution better than 20 lp/mm, temporal resolution of 12 ps, line-spread function of 40 μm (fwhm), contrast transfer ratio (CTR) of 60% at 10 lp/mm, and system sensitivity of 16 CCD electrons per photoelectron. A dynamic range of 60 for a 2 ns window is determined from system noise, linearity and sensitivity measurements.

Work performed under the auspices of the U.S. DOE by UC, LLNL contract No. W-7405-Eng-48.

1. INTRODUCTION

The Lawrence Livermore National Laboratory (LLNL) Laser Programs built more than 30 high-speed optical streak cameras[1] in the 1970s and 1980s. These cameras have provided the Inertial Confinement Fusion (ICF) Program with high-speed recording capability for nearly 30 years. The cameras record streak images for a variety of laser[2], x-ray[3], and particle instruments[4] that require temporal resolutions approaching 10 ps. The cameras use a large-format (40-mm diameter) RCA C73435 streak tube directly coupled to a microchannel-plate image-intensifier tube (MCP IIT). Before 1987, streak camera images were captured on hard-film at the output of the IIT. In the mid 1980s, 15 cameras that were built for the Nova laser project incorporated CCD readouts in place of the earlier film packs. A lens relayed the IIT output image to the CCD because direct fiber-optic (FO) coupling was not yet reliable.

Unfortunately, the streak cameras are becoming difficult to maintain because several of their components, including the streak tube and the IIT, are no longer available. Furthermore, the National Ignition Facility (NIF) projects a need for approximately 50 optical streak cameras. The work reported in this article is related to the ICF Program's search for optical streak cameras whose performance is equivalent to or better than the original Livermore design.

The Laboratory for Laser Energetics (LLE) at the University of Rochester is leading an effort to develop a modern, totally automated streak camera. Their design incorporates many years of experience using Livermore cameras and cameras of a more recent LLE design that they developed for power balance measurements. Performance requirements for the new camera are driven by the needs of LLE's OMEGA Laser

Facility. These needs are quite similar to those of the NIF. The performance of a prototype camera has been measured at Livermore. Preliminary results of these measurements are reported in this article.

2. THE ROCHESTER OPTICAL STREAK CAMERA SYSTEM

The streak camera characterized for this article is called the ROSS (Rochester Optical Streak System). It is based on the Photonis P-510 streak tube that shares many similarities with the RCA C73435. Each tube has a large format (40-mm diameter), a slotted extraction grid, a photocathode-to-anode voltage of 15 kV, similar internal electrode structures, and similar lengths. Perhaps the most significant tube difference is the spacing between photocathode and extraction grid, 5 mm for the P-510 versus 7 mm for the C73435. For identical photocathode and extraction grid voltages, the higher electric field at the P-510 photocathode allows a higher linear current density to be extracted and reduces electron transit time dispersion through the tube.

Streak tubes can have a slotted or a mesh type extraction grid. A slotted grid (a true slot in the P-510, parallel wires in the C73435) provides an advantage. An electrostatic lens formed by the slot coupled with the electrostatic lens formed by the focus grid allows electrons from a relatively wide strip (0.5 to 1 mm) of the photocathode to be focused to a narrow line at the output of the tube. Because image width for mesh type tubes is simply proportional to the width of the illuminated strip, their input slit widths are typically < 100 μm to maintain reasonable time resolution. A streak tube with a slotted extraction grid can have 10 times more usable photocathode area than a mesh type tube. Thus it can have 10 times more sensitivity and support 10 times more current.

The ROSS does not use a MCP IIT. In the Livermore camera, a MCP IIT provides enough gain so that the signal from a single photoelectron is greater than the image noise. It has long been known that the IIT also limits the camera's spatial resolution[5]. The ROSS, like the earlier LLE camera, couples the streak tube image directly to a CCD through a coherent FO coupler. The low noise, improved efficiency, and high amplifier gain of modern CCDs and the efficiency of FO couplers now allow single photoelectrons to produce signals greater than the image noise without needing an IIT. The ROSS uses a Spectral Instrument's SI-800 CCD camera with a 2Kx2K EEV back-illuminated CCD with 13 μm pixels and a 1:1 FO coupler.

The ROSS consists of two distinct parts: the main streak camera module and an optics module. The camera module contains the streak tube, CCD readout, power supplies, and digital interface electronics; the optics module contains calibration light sources, slits, filters, and imaging optics for safely coupling optical input signals to the streak tube. The camera module has been designed and a prototype built. Design of the optics module is nearing completion, but a prototype is not yet available. All data acquired for this article used the slit and lens arrangement from a Livermore streak camera to couple optical signals into the ROSS prototype containing a P-510 tube with an S-20 photocathode. The goal of this work was to understand the performance of the streak camera module, not the optics module.

3. STREAK CAMERA CHARACTERIZATION

Characterization evaluates performance parameters that provide a detailed understanding of how a camera performs under a variety of operating conditions.

Characterization helps determine the optimum camera configuration and the best component settings. In this study, we evaluated (1) magnification, (2) spatial resolution, (3) temporal resolution, (4) noise, (5) sensitivity, (6) linearity, and (7) dynamic range. For this work, the camera was set up using techniques similar to those used with Livermore cameras. It is probable that additional work with the ROSS will lead to improvements in performance. Unless noted otherwise, measurements reported here used a 1-mm wide slit (in temporal direction) and a collimated, 0.53-μm laser beam. Collimated light creates a large depth of focus and eliminates the input optic as a factor in resolution measurements.

3.1 Magnification and Field of View

Magnification and field-of-view (FOV) are measured with collimated laser light passing through a mask of 10-μm slits evenly spaced 1.5 mm apart. Data were recorded with the mask placed in two different positions. First, the mask was placed against the streak tube input window to give a direct measurement of the tube's spatial magnification. Then the mask was placed at the slit plane of the system to measure magnification of the entire system, input optics plus streak tube. Measured streak tube magnification matches the tube spec of 1.3. The input optics has an additional magnification of 1.16 giving the test system a magnification of 1.5. Since the final optics module will have 1-to-1 imaging, all measurements in this article are referred to the streak tube photocathode. A single pixel at the CCD views 10 μm of the streak camera's photocathode. The camera's FOV is limited to 20.5 mm by the CCD. The CCD views a 26.6 mm square of the 40 mm diameter image. A slight increased in FOV could be achieved with a larger CCD array.

3.2 Spatial resolution

A line-spread function (LSF) and a contrast transfer function (CTF) are alternate ways to describe spatial resolution. In this work we measured the system LSF, then calculated the CTF by convolving the LSF with square-wave masks at various frequencies. Images recorded with Ronchi ruling masks confirm the accuracy of the LSF measurement and CTF calculation.

Figures 1a shows the camera's LSF measured using a 15-ns laser pulse entering the camera through a 10-µm wide spatial mask. Spatial resolution referred to the photocathode is 40 µm (fwhm). The LSF appears as a sharp spike rising a factor of 400 above the noise and broadens only slightly more than a Gaussian of the same width. The slightly asymmetric shape has not investigated and is likely an artifact of our measurement technique. The calculated CTF (figure 1b) shows a 60% contrast transfer ratio (CTR) at 10 lp/mm and a limiting visual resolution (5% CTR) > 20 lp/mm.

CTR measurements made at 6 and 10 lp/mm to confirm the validity of the CTF calculation. Measurements used a Ronchi ruling placed along the streak camera slit and illuminated by a collimated laser beam. Analysis consists of determining envelope functions for the peaks and for the valleys of spatial lineouts. Then the CTR is calculated from these functions. This technique allows measurement of the CTR without requiring a spatially uniform illumination of the input slit. CTRs of 93% and 68% were measured at spatial frequencies of 5.2 and 8.6 lp/mm, respectively, in agreement with the calculated CTF (figures 1c & 1d).

In figure 2, a contour plot shows the position dependence of the spatial resolution for the entire streak camera image. Data was recorded using a mask with 10-μm openings every 1.5 mm. The fwhm is determined at various spatial positions along the parallel time lines. Contour plots are presented for input slit widths of 1 mm and 100 μm. Improved spatial resolution is obtained with the narrow slit, but dynamic range is reduced by about 5. (For the P-510 tube, we found that only the central 550 μm of the 1 mm region illuminated by the laser actually contributes to the tube's signal).

3.3 Temporal resolution

Three factors influence time resolution: transit-time spread of electrons moving between photocathode and output plate, sweep rate of the electron beam, and slit image width in the temporal direction. A simple static measurement in which the deflection plates are grounded and the tube illuminated with either a laser pulse or a DC light source provides an excellent estimate for camera temporal resolution. The fwhm Δx of the static line represents the best temporal resolution (in pixels) possible with the camera. To form a good estimate for streak camera temporal resolution simply multiply Δx by the dwell time (ps/pix) of the sweep obtained from a time base calibration and add the result in quadrature with the electron transit-time spread (typically 7 to 10 ps). For this camera temporal resolutions of 12, 22, and 45 ps fwhm are estimated for the 2, 6, and 12 ns sweep windows. Resolution was checked for consistency by measuring the width of a short (45 ps fwhm) laser pulse at each sweep speed.

The streak camera allows DC voltages to be applied to the deflection plates. We generated an image in which a series of voltage steps were applied to the deflection plates. The resulting image is a set of constant time lines each of which can be analyzed along its spatial extent. Figure 3 shows a contour map of the position dependence of the temporal resolution (in pixels) in the streak camera image. With a 100 μm slit, 90% of the image has < 5-pixel (fwhm) resolution.

3.4 Noise and Gain

Knowledge of camera noise and gain are needed for understanding streak camera dynamic range. Noise establishes the weakest signal that a camera can record. Gain determines whether or not a single event can be seen. Background images provide information about read noise, dark current noise, and signal threshold. They allow us to verify the noise characteristics reported by the CCD manufacturer and to determine if additional noise is introduced by the other streak camera components. For this work, we simply measured image noise for 2 second exposures with different binning configurations (no binning, 2x2, 3x3, and 4x4). For no binning (1x1) we measured system a noise of 5.13 e^-, nearly identical to the CCD specification of 5.05 e^-. This indicates that nearly all camera noise comes from the CCD readout. Dark current in the CCD causes a slight increase in CCD noise when pixels are binned for readout: 5.97, 6.67, and 7.9 e- respectively for 2x2, 3x3 and 4x4 binning.

Photocathode sensitivity (QE) tells how well the photocathode converts incident light to photoelectrons. The manufacturer's data show this camera's sensitivity to be 0.025 amps/watt at a wavelength of 0.530 μm. Gain describes how well each signal photoelectron is amplified and converted into CCD electrons. System gain was measured by illuminating a 3-mm by 0.5 mm region of the photocathode with a 18-ns long, 0.53

μm, square pulses of known energy and recording the images. The number of ADUs in a recorded signal divided by the incident energy generating the signal gives the ADUs/nJ. Using the photocathode sensitivity (amps/watt) and the CCD gain (1.09 CCD e^- /ADUs) allows conversion of this value to CCD e^- / pe^-. For this camera we measured 16 CCD e^- per pe^-.

3.5 Dynamic Range

The concept of dynamic range is relatively simple: divide the maximum usable signal by the minimum observable signal. Unfortunately, problems quickly arise with the definitions used for the minimum and maximum signal. For this work, the dynamic range is determined per streak camera resolution element (4 CCD pixels in space and 8 CCD pixels in time). We consider the maximum usable signal to be that at which the temporal pulse broadens by 20%. The maximum signal depends on sweep speed. When the streak tube is the limiting element, temporal broadening can be correlated with the Child-Langmuir (C-L) space-charge-limited current at the photocathode. A 20% broadening occurs at ~10% of the C-L current.

To determine the maximum signals to be used for dynamic range calculations, temporal signals were recorded for 50-ps (fwhm) laser pulses were recorded with 2 ns, 6 ns, and 12-ns streak camera windows. Figure 4 shows temporal fwhm versus input tube current.

We use signal-to-noise ratio (SNR) per image resolution element as a figure-of-merit to help establish dynamic range. SNR can be written as:

$$SNR = s^2N / [s^2N + (s/s_b)^2\sigma_b^2/C^2]^{1/2}, \qquad (1)$$

where s^2 is the number of detector pixels in a resolution element (32 for this camera), N is the number of photoelectrons per detector pixel, s_b^2 is the number of detector pixels in a super pixel binned before readout (i.e. 1, 4, 9, and 16 for unbinned, 2x2, 3x3 and 4x4 respectively), σ_b is the noise associated with recording a single binned pixel, and C is the system sensitivity in CCD electrons per photoelectron. SNR can be increase by (1) increasing s^2 for more signal averaging, (2) increasing N by reducing camera sweep speed, (3) increasing C by improving CCD efficiency or increasing streak tube light output, and (4) decreasing system noise σ_b with an improved CCD.

Figure 5 shows SNR versus N for this camera using various CCD binning. The value of N corresponding to 10% of the C-L current is 60, 138, and 291, respectively, for time windows of 2, 6, and 12 ns. The increase in N occurs because the peak current integrates longer at the slower sweeps. At low values of N, the effect of CCD noise is noticeable. Going from 1x1 to 2x2 binning produces a significant improvement in SNR by primarily reducing the effect of CCD read noise. Additional binning provides little benefit for this camera. The minimum signal is taken at a SNR of 5. At just 1 photoelectron per detector pixel signal begins to rise above the background noise. Thus the dynamic range for the camera is 60, 138, and 291 for sweep speeds corresponding to time windows of 2, 6, and 12 ns, respectively. Note, there are 32 CCD elements per image resolution element and that these CCD elements are binned 2x2 before readout. Therefore, the weakest observable signal for this camera (N = 1) actually has 32 photoelectrons generated in an image resolution element.

4. DISCUSSION

The new streak camera performs very well and appears to satisfy most NIF optical streak camera requirements. Magnification, FOV, temporal resolution, and sweep linearity are comparable to the current LLNL camera. The ROSS, however, excels in spatial resolution with a 40-μm (fwhm) LSF and CTF limiting visual > 20 lp/mm, about 3 times better than the LLNL camera's 120 μm (fwhm) and 9 lp/mm. By excluding an IIT from the ROSS design, the main resolution-broadening component has been eliminated. The P-510 tube with its improved current and the efficient back-thinned CCD with fiber-optic coupler provide the camera with reasonable a gain of 16 CCD electrons per photoelectron relative to the ~6 e- of noise per binned pixel. The ROSS dynamic range has not yet been carefully compared with the LLNL camera, as image resolution elements are different sizes. This will be the next step in our analysis.

ACKNOWLEDGMENTS

The authors thank the talented and creative streak camera design team at LLE for their help in fielding the prototype camera at Livermore. Wade Bittle, Mark Donovan, and Keith Ebbecke provided electrical engineering support, and Gregory Antonini(of LLNL on assignment at LLE), Andrew Dillenbeck, and Lorie Hayes for mechanical engineering support. This work was performed under the auspices of the U.S. Department of Energy by University of California Lawrence Livermore National Laboratory under Contract No. W-7405-ENG-48.

FIGURE CAPTIONS

Figure 1. Spatial resolution. (a) Line spread function, (b) contrast transfer function, (c) portion of image taken with 10 lp/mm Ronchi ruling mask, and (d) plot amplitude versus spatial position in Ronchi ruling image.

Figure 2. Contour map shows spatial dependence of spatial resolution. Left side is for 1-mm wide slit, right side is for 100-µm slit.

Figure 3. Contour map shows spatial dependence of time resolution for 100-µm slit.

Figure 4. Temporal broadening of laser pulse versus streak tube current for three sweep speeds.

Figure 5. SNR versus photoelectrons per CCD pixel. SNR computed for ROSS streak camera using equation 1 with $s^2 = 32$, $s_b^2 = 1$ (2, 9, & 16), $C = 16$, and σ_b^2 values given in article text.

(a) (b) (c & d)

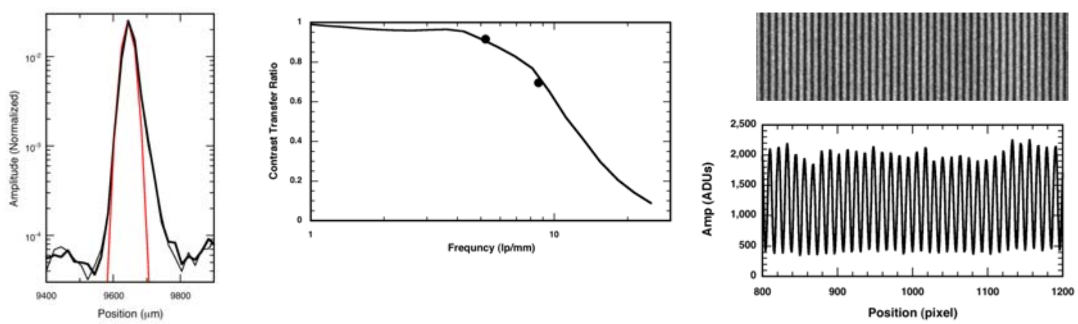

Figure 1.

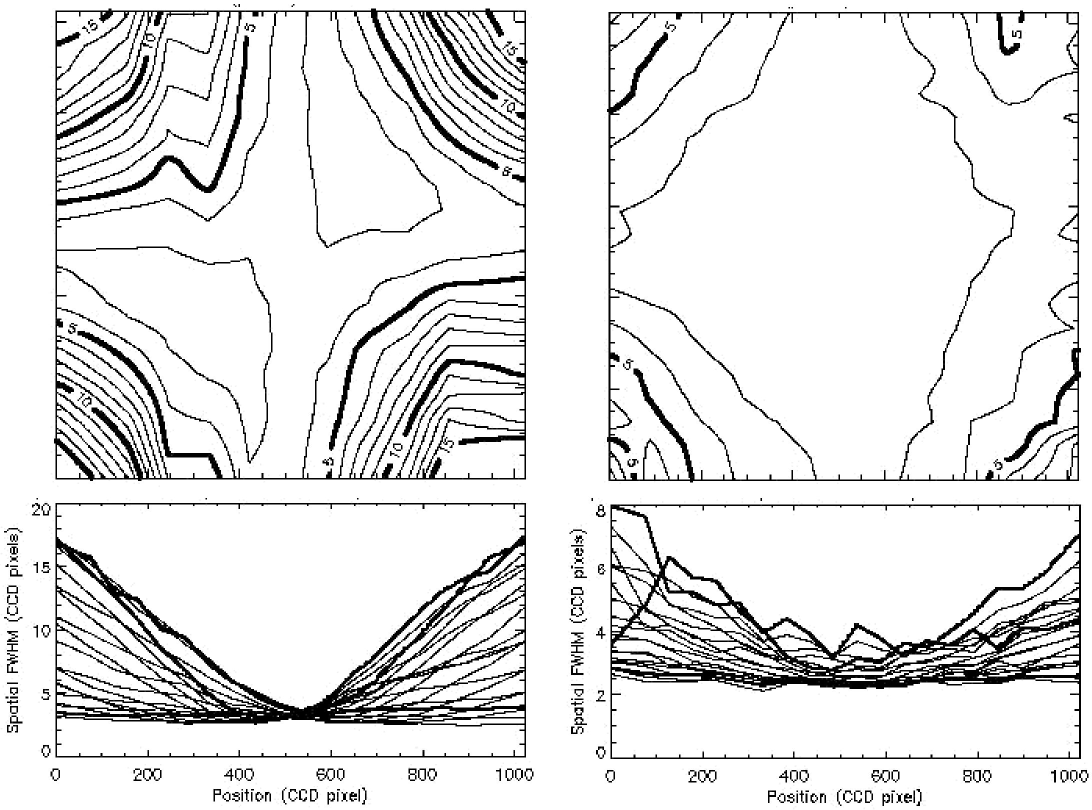
Spatial FWHM (CCD pixels)
Position (CCD pixel)
Spatial FWHM (CCD pixels)
Position (CCD pixel)

Figure 2.

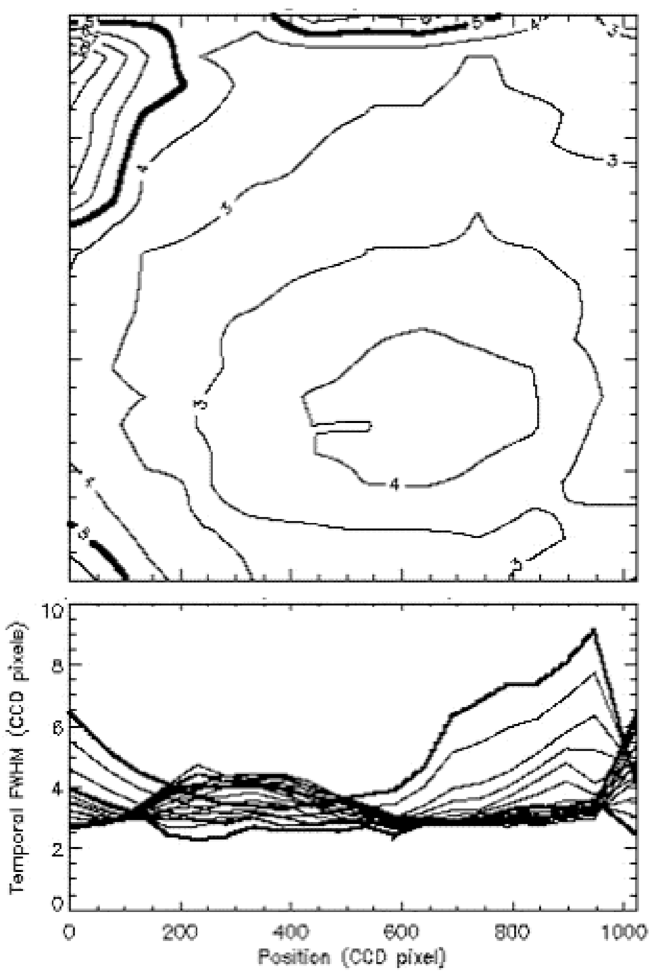
Temporal FWHM (CCD pixels)
Position (CCD pixel)
0
200
400
600
800
1000
2
4
6
8
10

Figure 3.

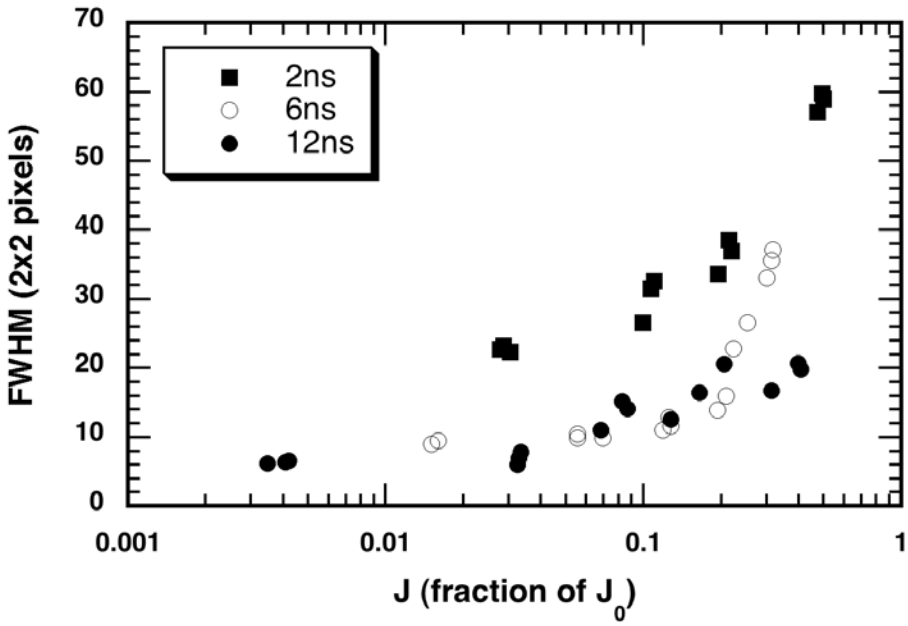
70
60
50
40
30
20
10
0
FWHM (2x2 pixels)
2ns
6ns
12ns
0.001
0.01
0.1
1
J (fraction of J0)

Figure 4.

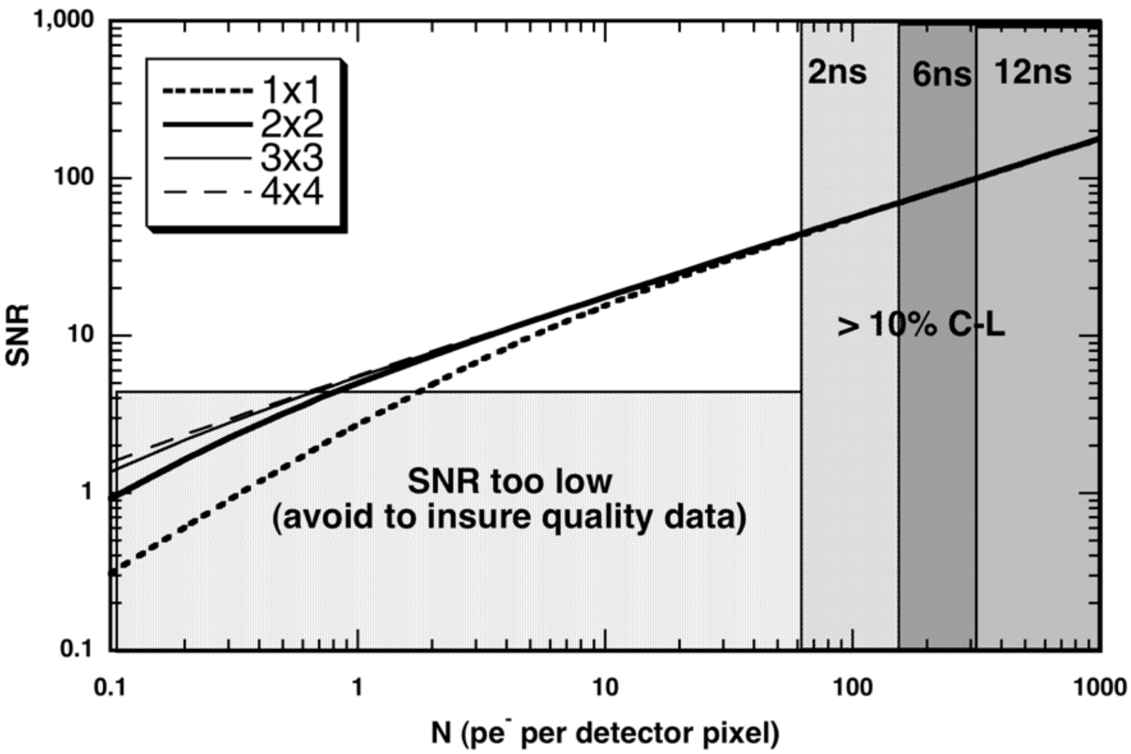
1x1
2x2
3x3
4x4
2ns
6ns
12ns
> 10% C-L
SNR too low
(avoid to insure quality data)
SNR
N (pe⁻ per detector pixel)
1,000
100
10
1
0.1
0.1
1
10
100
1000

Figure 5.

REFERENCES

[1] S. W. Thomas, J. W. Houghton, G. R. Tripp, and L. W. Coleman, "The LLL compact 10 ps streak camera—1974 update," Proc. of 11th Int'l Cong. on High Speed Photography, London, p. 101 (1974).

[2] R. A. Lerche, "Timing between streak cameras with a precision of 10 ps," Proc. of SPIE Conference on Ultrahigh- and High-Speed Photography, Videography, Photonics, and Velocimetry '90, SPIE Vol. **1346**, pp. 376-383 (1990).

[3] D. T. Attwood, R. L. Kauffman, G. L. Straddling, H. L. Medecki, R. A. Lerche, L. W. Coleman, E. L. Pierce, S. W. Thomas, D. E. Campbell, J. Noonan, G. R. Tripp, R. J. Schnetz, and G. E. Phillips, "Picosecond X-Ray Measurements from 100 eV to 30 keV", Proc. of XIV International Congress on High Speed Photography and Photonics, Moscow (1980).

[4] R. A. Lerche, D. W. Phillion, and G. W. Tietbohl, "Neutron detector for fusion reaction-rate measurements," Proc. of SPIE Conference on Ultrahigh- and High-Speed Photography, Videography, and Photonics, '93, SPIE Vol. **2002**, pp. 153-161 (1993).

[5] J. D. Wiedwald and R. J. Hertel, "Veiling Glare in the ITT F4113 Image Intensifier", Proc. of SPIE Conference on High Speed Photography, Videography, and Photonics VI, SPIE Vol. **981**, pp. 154-160 (1988).